Beam driven electron-acoustic waves in Auroral region of magnetosphere with superthermal trapped electrons

R. Jahangir*,[1] S. Ali,[1] and B. Eliasson[2]
[1)]*National Centre for Physics, Shahdara Valley Road, Islamabad, Pakistan*
[2)]*SUPA, Physics Department, University of Strathclyde, Glasgow, United Kingdom*

(*Electronic mail: rabiaj@ncp.edu.pk)

(Dated: 30 December 2024)

The propagation characteristics of nonlinear electron-acoustic (EA) waves are studied in a four component magnetoplasma, containing inertial cold electrons, warm drifting beam electrons, trapped superthermal hot electrons, and static ions. A linear dispersion relation for EA waves is derived to analyze the impact of electron superthermality on the $\omega - k$ relation. For nonlinear analysis, a reductive perturbation formalism is adopted to solve the set of model equations in the form of a trapped Zakharov-Kuznetsov (tZK) equation. The latter is analyzed to determine the solitary structures in terms of phase portraits and exact soliton solutions showing the impact of electron trapping efficiency (γ), hot electron superthermality (κ), drifting speed, temperature and density of beam electrons, and temperature and density of cold electrons, using typical parameters from the short-duration burst of broad-band electrostatic noise emissions observed by the Viking spacecraft in the auroral region. The solitary structures propagate as positive potential pulses and become modified with superthermal trapped electrons, leading to hole (hump) in cold (hot) electron density excitations. The electric field structures of the EA waves are found to be in exact agreement with the observed solitary structures in the auroral region. It is observed that electric field strength associated with these waves decreases as the magnetic field effect increases. The present model can be used to understand the transport of energy and momentum between plasma particles and to comprehend magnetic reconnection region in magnetopause, where two-temperature electrons and large-amplitude parallel electrostatic waves have been reported by Magnetopause Multiscale observations.

I. INTRODUCTION

Electron-acoustic (EA) waves have been widely studied since their first investigation in 1961 by Fried and Gould who studied numerical solutions of the electrostatic Vlasov dispersion relation[1]. The waves were later confirmed experimentally in 1972 by Henry and Treguier in an unmagnetized plasma[2]. The EA waves essentially require two populations of electrons with different temperatures and number densities in the static background of ions such that $T_h \geq 10T_c$ and $0.2 < n_c/n_e < 0.8$, where c, h and e refer to cold, hot and total electrons[3]. These waves are electrostatic in nature and have been observed by many missions, e.g., S3-3 and THEMIS in the auroral region[4,5], POLAR in the polar cusp[6], Viking and FAST satellites in the polar cusp boundary layer[7–9], GEOTAIL in the plasma sheet boundary layer[10], CLUSTER in the Earth's magnetosphere/magnetopause[11,12], etc. The observations show large bipolar electric field component parallel to the magnetic field, in the range from a few mV/m to $100mV/m$, observed as broadband electrostatic noise (BEN) in frequency domain. Scarf et al.[13] and Gurnett et al.[14] reported the initial measurements of BEN in frequency domain using IMP 7 and 8 satellite data, later reported by many more researchers. By studying the waveforms, these emissions were interpreted as electrostatic solitary waves[15–17]. The existence of EA waves have also been reported by Magnetospheric Multiscale (MMS) observations during asymmetric magnetic reconnection at the Earth magnetopause[18,19].

The *trapping of plasma particles* in electrostatic waves is a peculiar phenomenon, in which plasma particles are trapped, showing back and forth oscillations in a finite region of phase space. Several distinct features of plasma waves have been discussed in the past by taking into account the particle trapping effect via numerical simulations[20,21] and laboratory experiments, investigating the basics of electron phase space vortices[22] and holes propagation in magnetoplasma column[23]. Space observations have confirmed the presence of solitary structures as electron hole modes at the Earth magnetopause[24] and electron phase space holes in the upward and downward current regions of the aurora[25,26]. Recent observations[27] by MMS have identified the large-amplitude bipolar electric field structures with trapped electrons in electron phase space holes.

In 1957, Bernstein, Greene, and Kruskal[28] analytically investigated the nonlinear properties of the electrostatic waves with particle trapping effects. Later, new equilibrium solutions have been analyzed using trapped/vortex-like distribution[29]. Small-amplitude ion-acoustic waves have also been described by the help of Korteweg de Vries (KdV)-like Schamel equation[30], showing a fractional nonlinearity caused by the trapped electrons[31]. Mamun and co-workers investigated EA waves with vortex electron distribution both in unmagnetized[32] and magnetized[33] plasmas. They expressed the nonlinear EA waves as positive potential excitations in the presence of a hole/dip in the cold electron number density. Recently, Rufai et. al.[34] discussed various properties of finite-amplitude EA waves in the electron diffusion region, obtaining a trapped KdV equation to show the propagation of EA waves at supersonic speeds. On the other hand, EA waves with a transverse distortion **were** analyzed in a cylindrical geometry with vortex electron distribution[35] **and revealed an** exact analytical solution for modified cylindrical Kadomtsev-Petviashvili (CKP) equation. In addition, the trapped Zakharov-Kuznetsov Burger's (tZKB) equation has been derived by Guo et. al.[36] for studying shock waves in

This is a peer-reviewed, accepted manuscript of the following paper: Jahangir, R., Ali, S., & Eliasson, B. (2025). Beam-driven electron-acoustic waves in auroral region of magnetosphere with superthermal trapped electrons. Physics of Fluids, 37(2), Article 027108. https://doi.org/10.1063/5.0249424

magnetized ionic-pair plasmas.

Apart from the formation of phase space holes due to particle trapping, *particle superthermality* is caused by energetic plasma particles and cannot be dealt with the Maxwell particle distribution. In such a situation, the use of a vortex-like/trapped non-isothermal distribution[37] could be an adequate choice for investigating the wave phenomenon and plasma instabilities as alternative scheme in describing the phase space holes. In this perspective, Williams et. al.[38] have introduced particle trapping in a kappa-distributed plasma and solved the KdV-like Schamel equation for planar IA solitons with superthermal-trapped electrons and cold ions. Sultana et. al.[39] developed a model for oblique propagation of EA waves with trapped superthermal electrons in a magnetized plasma.

In the laboratory, EA waves are often excited by lasers[40] or by the electron beams and therefore the field aligned electron beam may act as a source of energy for excitation of EA waves in the presence of two temperature electron populations. Berthomier et. al.[41] described the properties of EA waves with the beam electrons in a plasma system. They found that a non-zero streaming velocity of the beam electrons generates a new class of the EA waves. They also examined critical conditions in terms of temperature and density for the beam electrons in which the electron density holes appear due to the presence of cold electrons. The study was later extended by including higher order nonlinearities with the electron beam and hot electron vortex distribution, strongly modifying the wave amplitudes and widths of the solitonic structures[42]. Singh et. al.[43] have explained the EA wave characteristics in a magnetoplasma with nonthermal electrons in the presence of electron beam. They applied their model to numerically analyze the auroral plasmas observed by the Viking satellite.

Over recent years, bifurcation analysis of dynamical systems has been performed by solving nonlinear partial differential equation, which has attracted lots of interest in the plasma physics community. Bifurcation stands for a significant sudden change in the dynamics of the system, which is subjected to a parametric variation. The phase plane portraits provides a qualitative analysis of a dynamical system, identifying the trajectories and equilibrium points for the stability within the system. Kumar et al.[44] utilized the bifurcation theory and investigated the properties of solitary and travelling waves by solving the Kadomtsev-Petviashili (KP) equation for dust-ion-acoustic waves in a magnetoplasma. Later, this theory for the small-amplitude nonlinear waves has been extended to a number of nonlinear partial differential equations including the modified KP equation[45], Zakharov-Kuznetsov (ZK) equation[46], trapped KdV equation[47], Burgers equation[48], Burgers-type equation with quartic nonlinearity[49], etc.

The motivation of this work is manyfold: Firstly, it delves into the significance of the magnetic field, which plays a crucial role in altering the amplitudes of electric fields for electrostatic waves. Secondly, the inclusion of energetic particles, specifically superthermal trapped hot electrons, provides a more realistic depiction of the auroral region. Lastly, the analysis of phase portraits associated with the tZK solitons in the context of plasma systems is a novel contribution. These research gaps have spurred the modeling of EA waves in a magnetized plasma, allowing for a comprehensive investigation of the linear and nonlinear properties of these waves, taking into account superthermal trapped and beam electrons. The model's findings are analyzed both analytically and numerically for the Earth's magnetosphere and compared with observational data.

The paper is organized as follows. Section II begins with the physical model to study EA solitary waves, containing fluid equations for inertial cold and beam electrons with hot superthermal trapped electrons, and static ions. Within the framework of reductive perturbation technique, a trapped Zakharov-Kuznetsov (tZK) equation is derived in Sec. III. The qualitative and quantitative analyses, in terms of Sagdeev potential and localized soliton solution with electric field components, are presented in Secs. IV and V, respectively. Section VI presents numerical findings, studying nonlinear EA waves in the context of BEN emission in the dayside auroral zone. Sec. VII summarizes the main results of this article.

II. MODEL FOR ELECTRON-ACOUSTIC (EA) WAVES

We study small but finite amplitude electron-acoustic (EA) waves in a magnetized, homogeneous plasma, comprising inertial cold electrons, superthermal hot trapped electrons, and stationary ions with a warm drifting electron beam. The wave propagates in a three-dimensional space along the $x-$, $y-$ and $z-$axes, namely, $\nabla = (\partial/\partial x, \partial/\partial y, \partial/\partial z)$. The plasma holds an equilibrium quasi-neutrality condition of the form $n_{h0} + n_{c0} + n_{b0} = n_{i0}$ and is subjected to a magnetic field in the $z-$axis, i.e., $\mathbf{B} = B_0\hat{z}$, where B_0 is the strength of magnetic field, $\hat{z}$ is the unit vector along the z-axis, and n_{s0} is the equilibrium number density of the each species (s equals h for hot electrons, c for cold electrons, b for beam electrons and i for positive ions). It is also assumed that there is a small finite temperature of the cold electrons (viz., $T_h \geq 10T_c$)[3] such that the wave is not Landau damped. The linear and nonlinear dynamics of the EA waves in a magnetoplasma is governed by the following normalized continuity, momentum, thermodynamical equation of state and Poisson equations, respectively.

$$\frac{\partial n_j}{\partial t} + \frac{\partial}{\partial x}(n_j v_{jx}) + \frac{\partial}{\partial y}(n_j v_{jy}) + \frac{\partial}{\partial z}(n_j v_{jz}) = 0, \quad (1)$$

$$\left(\frac{\partial}{\partial t} + \mathbf{v}_j.\nabla\right)\mathbf{v}_j = \alpha\nabla\phi - \Omega\mathbf{v}_j \times \hat{z} - \alpha\frac{\sigma_j}{n_j}\nabla p_j, \quad (2)$$

$$\left(\frac{\partial}{\partial t} + \mathbf{v}_j.\nabla\right)p_j + 3p_j\nabla.\mathbf{v}_j = 0, \quad (3)$$

and

$$\nabla^2\phi = n_h + \frac{1}{\alpha}n_c + \frac{1}{\beta}n_b - \left(1 + \frac{1}{\alpha} + \frac{1}{\beta}\right), \quad (4)$$

with the ratios

$$\alpha=\frac{n_{h0}}{n_{c0}},\beta=\frac{n_{h0}}{n_{b0}},\sigma_c=\frac{T_c}{T_h},\sigma_b=\frac{T_b}{T_h}\text{ , and }\Omega=\frac{\omega_{ce}}{\omega_{pc}}. \quad (5)$$

where $j(=c,b)$ stands for cold and beam electrons, $\omega_{pc}=\left(4\pi e^2 n_{c0}/m_e\right)^{1/2}$ and $\omega_{ce}=\omega_{cb}=eB_0/m_e c$ are the cold electron plasma oscillation frequency and cyclotron frequency, respectively. In the above equations, $n_{h,c,b}$ represent the number densities of the hot, cold and beam electrons and are scaled by their corresponding equilibrium values n_{h0}, n_{c0} and n_{b0}, respectively. The cold and beam electron fluid velocities $\mathbf{v}_{c,b}$ are normalized by the electron-acoustic speed $c_{ea}=\left(T_h/\alpha m_e\right)^{1/2}$, where T_h is the hot electron temperature (in energy units), ϕ is the electrostatic potential normalized by T_h/e, while p_j is the pressure normalized by $n_{j0}T_j$. Furthermore, the space and time coordinates are scaled by the hot-electron Debye length $\lambda_{Dh}=\left(T_h/4\pi e^2 n_{h0}\right)^{1/2}$ and the inverse cold electron plasma frequency ω_{pc}, respectively. Since the superthermal hot electrons are assumed to be trapped in the wave potential, so they are described by the following trapped kappa distribution function[38]:

$$f_{Th}^{\kappa}(\upsilon,\phi)=\frac{n_{h0}}{\sqrt{\pi\kappa\theta^2}}\frac{\Gamma(\kappa)}{\Gamma(\kappa-1/2)}\left[1+\gamma\frac{\frac{m_h\upsilon^2}{2k_BT_h}-\frac{e\phi}{k_BT_h}}{\kappa-3/2}\right]^{-\kappa}. \quad (6)$$

For $\gamma=1$ in Eq. (6), the distribution function $f_{Fh}^{\kappa}(\upsilon,\phi)$ is obtained for superthermal free electrons. The parameter $\gamma(=T_{hF}/T_{hT})$ identifies the efficiency of electron trapping, where T_{hF} and T_{hT} denote the free and trapped hot electron temperatures. Note that the limit $\gamma=0$ determines a plateau and $\gamma>0$ ($\gamma<0$) describes the hump (dip) in the distribution function of hot electrons[37]. On the other hand, the spectral index κ represents the highest electron superthermality effect at the lower bound $3/2$ and shows completely the Maxwellian behavior at infinity, while an intermediate domain determines the impact of superthermal electrons. The gamma function is denoted by the symbol Γ.

To calculate number density for superthermal (hot) trapped electrons, we first decompose the total distribution function into the trapped and free distribution functions $[i.e., f_h^{\kappa}(\upsilon,\phi)=f_{Th}^{\kappa}(\upsilon,\phi)+f_{Fh}^{\kappa}(\upsilon,\phi)]$ and define integration limits, as

$$n_h=\int_{-\infty}^{\infty}f_h^{\kappa}(\upsilon,\phi)\,d\upsilon\equiv\int_{-\infty}^{-\sqrt{2e\phi/k_BT_h}}f_{Fh}^{\kappa}(\upsilon,\phi)\,d\upsilon + \int_{-\sqrt{2e\phi/k_BT_h}}^{\sqrt{2e\phi/k_BT_h}}f_{Th}^{\kappa}(\upsilon,\phi)\,d\upsilon+\int_{\sqrt{2e\phi/k_BT_h}}^{\infty}f_{Fh}^{\kappa}(\upsilon,\phi)\,d\upsilon, \quad (7)$$

Now performing integrations in the above equation and expanding the potential ϕ by the Taylor expansion, one eventually arrives at an un-normalized density for superthermal trapped hot electrons[38], as

$$\frac{n_h}{n_{h0}}=1+A\frac{e\phi}{k_BT_h}+B\left(\frac{e\phi}{k_BT_h}\right)^{3/2}+C\left(\frac{e\phi}{k_BT_h}\right)^{2}+... \quad (8)$$

Equation (8) in a normalized form becomes as

$$n_h=1+A\phi+B\phi^{3/2}+C\phi^2... \quad (9)$$

with the following expansion coefficients

$$A=\frac{\kappa-1/2}{\kappa-3/2},\ B=-\frac{4(1-\gamma)}{3\sqrt{\pi}}\frac{\kappa\Gamma(\kappa)}{(\kappa-3/2)^{3/2}\Gamma(\kappa-1/2)}, \quad (10)$$

and

$$C=\frac{\kappa^2-1/4}{2(\kappa-3/2)^2}. \quad (11)$$

See that if $\gamma=1$, then the coefficient $B=0$ vanishes and consequently the effect of trapped electrons is ignored in Eq. (9). This immediately gives rise to the number density of superthermal hot electrons only. Upon further considering the limit $\kappa\to\infty$, we recover the standard Boltzmann (Maxwellian) density relation for hot electrons from Eq. (9). Conversely, if we only take into account the electron trapping effect, ignoring electron superthermality effect in Eq. (9), then Schamel's electron density[37] that causes fractional nonlinearity in Maxwellian-distributed plasma is recovered.

III. TRAPPED ZAKHAROV–KUZNETSOV EQUATION WITH BEAM ELECTRONS

To investigate the propagation properties of small-amplitude EA waves in a magnetoplasma, in the presence of superthermal electrons with a trapped population, cold electrons and beam electrons, we use the well-known reductive perturbation technique (RPT), in which all the dependent variables are expanded in powers of ε around the equilibrium values, whereas independent (i.e., space and time) coordinates are stretched in terms of new coordinates[50]. To express the propagation of a stable solitary structure in a particular direction, the wave is assumed to move along the $z-$direction that dominates over the perturbations in $y-$ and $x-$ directions. Thus, one can define the required stretchings in this form:

$$\xi=\varepsilon^{1/4}x,\ \eta=\varepsilon^{1/4}y,\ \chi=\varepsilon^{1/4}(z-\lambda t),\text{ and }\tau=\varepsilon^{3/4}t, \quad (12)$$

where λ represents the phase speed of the wave normalized by c_{ea} and ε is the dimensionless parameter ($0<\varepsilon\leq 1$) describing the small amplitude of nonlinearity. Similarly, using the RPT, all the dependent variables n_c, n_b, v_{cx}, v_{bx}, v_{cy}, v_{by}, v_{cz}, v_{bz}, p_c, p_b and ϕ, are expanded in terms of ε as

$$\begin{pmatrix}n_j\\v_{jx}\\v_{jy}\\v_{jz}\\p_j\\\phi\end{pmatrix}=\begin{pmatrix}1\\0\\0\\v_{j0}\\1\\0\end{pmatrix}+\begin{pmatrix}\varepsilon n_{j1}+\varepsilon^{3/2}n_{j2}+...\\\varepsilon^{5/4}v_{jx1}+\varepsilon^{3/2}v_{jx2}+...\\\varepsilon^{5/4}v_{jy1}+\varepsilon^{3/2}v_{jy2}+...\\\varepsilon v_{jz1}+\varepsilon^{3/2}v_{jz2}+...\\\varepsilon p_{j1}+\varepsilon^{3/2}p_{j2}+...\\\varepsilon\phi_1+\varepsilon^{3/2}\phi_2+...\end{pmatrix}. \quad (13)$$

Since we are assuming that velocity perturbations are weaker in the transverse direction compared to the velocity perturbations along the propagation direction, therefore, the transverse

velocity components are expressed in higher orders of ε relative to the parallel velocity component. Consequently, the powers of ε in the expansion of transverse and parallel velocity components [$v_{jx,jy}$ and v_{jz}] start with 5/4 and 1, respectively. The high (low) orders of ε correspond to weak (strong) velocity perturbations in the transverse direction (propagation direction). Similarly, it is also noted from (13) that only beam electrons stream along the parallel direction with a constant speed v_{b0}, while the streaming of cold electrons is neglected in this model, $v_{c0}=0$.

Now, employing Eqs. (12) and (13) into the governing Eqs. (1)-(4) along with (9), we get a set of equations for various orders of ε. The lowest–order (i.e.,$\varepsilon^{5/4}$-order) terms yield the following expressions:

$$(\lambda - v_{j0})\frac{\partial n_{j1}}{\partial \chi} = \frac{\partial v_{jz1}}{\partial \chi},$$

$$-(\lambda - v_{j0})\frac{\partial v_{jz1}}{\partial \chi} = \alpha\frac{\partial \phi_1}{\partial \chi} - \alpha\sigma_j\frac{\partial p_{j1}}{\partial \chi},$$

$$(\lambda - v_{j0})\frac{\partial p_{j1}}{\partial \chi} = 3\frac{\partial v_{jz1}}{\partial \chi},$$

$$\Omega v_{jx1} = -\alpha\frac{\partial \phi_1}{\partial \eta} + \alpha\sigma_j\frac{\partial p_{j1}}{\partial \eta},$$

and

$$\Omega v_{jy1} = \alpha\frac{\partial \phi_1}{\partial \xi} - \alpha\sigma_j\frac{\partial p_{j1}}{\partial \xi}. \tag{14}$$

The above set of equations represent the first order equations that can be solved simultaneously, obtaining the following linear dispersion relation

$$A - \frac{1}{\lambda^2 - 3\alpha\sigma_c} - \frac{\alpha}{\beta((\lambda - v_{b0})^2 - 3\alpha\sigma_b)} = 0. \tag{15}$$

This is a quartic equation in terms of the phase speed $\lambda = \omega/k$, indicating four distinct roots of the equation, two of which are positive while other two are negative[51]. The negative roots represent the wave propagation in the negative direction. The positive roots however, correspond to the slow and fast EA modes in the positive direction. Furthermore, as the roots are distinct, so the value of positive roots is greater than the value of negative roots. The above dispersion well-concurs with the previous result[42], highlighting a special case involving Schamel's distribution function with trapped Maxwellian electrons in the limit $\kappa \to \infty$. It may be noted from (15) that this dispersion relation does not include the trapping effect or parameter γ, and so the electron trapping does not affect the linear EA waves, only appearing through the fractional nonlinearity in the nonlinear systems. The dispersion relation is however modified by the electron superthermality index κ via A, as well as number densities and temperatures of all three electron populations and beam electrons (via v_{b0}). In the absence of beam electrons ($v_{b0} \to 0$ and $\beta \to \infty$), the dispersion relation reduces to $\lambda = \sqrt{3\alpha\sigma_c + 1/A}$, which is an agreement with the result of Mamun and Shukla[32] for neglecting cold electron temperature $T_c = 0$.

It is worth mentioning here that the frequency of EA waves intermediates the Langmuir and ion-acoustic wave frequencies, exhibiting an acoustic behavior. Due to smaller frequency of the EA waves compared to Langmuir waves, these waves can be studied within the framework of the reductive perturbation technique (RPT). This technique is often utilized to investigate weakly nonlinear waves that propagate on slow temporal and spatial scales. Accordingly, the wave amplitude or its shape gradually changes over a long distance or time. The RPT is applicable for the waves in the long wavelength limit, i.e., $k\lambda_{dh} << 1$. This means that the leading-order equations derived from the RPT give rise to non-dispersive waves in the linear limit, even though the original system is dispersive. The dispersive effects can be captured when higher orders of epsilon are included.

Figure 1 represents the linear characteristics of the EA waves

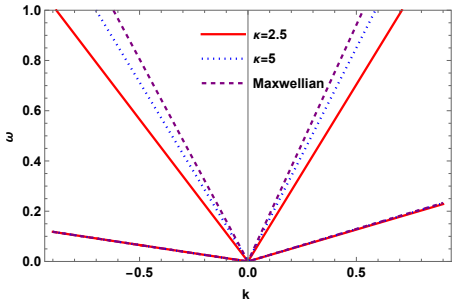

FIG. 1. The linear frequency ω of the EA waves changes with superthermal parameter κ. The numerical values such as α=4, β=2, v_{b0}=0.1, σ_c=0.001, σ_b=0.01 and γ=0.1 correspond to burst a of BEN emission.

via Eq. (15) and plots normalized wave frequency (ω/ω_{pc}) against the normalized wavenumber ($k\lambda_{Dh}$) for different values of superthermality index κ. It may be noted that trapping being a nonlinear phenomenon, does not affect the linear properties of the EA waves. Also observe that negative and positive slow modes do not get influenced by the superthermality parameter. Both positive and negative fast modes attain higher magnitudes for the higher values of κ. In other words, the phase speed of the wave reduces (increases) at high superthermality as compared with low superthermality. We, therefore, focus on the nonlinear properties of the fast positive EA mode later in our manuscript.

Now collection of next-order (i.e., $\varepsilon^{7/4}$-order) terms leads to the derivation of nonlinear equations containing the second order perturbed quantities in terms of first order perturbed quan-

tities, as

$$
\begin{aligned}
&-(\lambda - v_{j0})\frac{\partial n_{j2}}{\partial \chi} + \frac{\partial v_{jz2}}{\partial \chi} = -\frac{\partial n_{j1}}{\partial \tau} - \frac{\partial v_{jx2}}{\partial \xi} - \frac{\partial v_{jy2}}{\partial \eta},\\
&(\lambda - v_{j0})\frac{\partial v_{jz2}}{\partial \chi} + \alpha\frac{\partial \phi_2}{\partial \xi} - \alpha\sigma_j\frac{\partial p_{j2}}{\partial \chi} = \frac{\partial v_{jz1}}{\partial \tau},\\
&(\lambda - v_{j0})\frac{\partial p_{j2}}{\partial \xi} - 3\frac{\partial v_{jz2}}{\partial \chi} = \frac{\partial p_{j1}}{\partial \tau} - 3\frac{\partial v_{jx2}}{\partial \xi} - 3\frac{\partial v_{jy2}}{\partial \eta},\\
&(\lambda - v_{j0})\frac{\partial v_{jx1}}{\partial \chi} = \Omega v_{jy2},\\
&(\lambda - v_{j0})\frac{\partial v_{jy1}}{\partial \chi} = -\Omega v_{jx2},\\
&A\phi_2 + \frac{1}{\alpha}n_{c2} + \frac{1}{\beta}n_{b2} = \left(\frac{\partial^2}{\partial \xi^2} + \frac{\partial^2}{\partial \eta^2} + \frac{\partial^2}{\partial \chi^2}\right)\phi_1 - B\phi_1^{3/2}.
\end{aligned}
\tag{16}
$$

After some algebraic steps, expressions of (16) can be solved together to obtain the following simplified nPDE

$$
\frac{\partial \phi_1}{\partial \tau} + P\phi_1^{1/2}\frac{\partial \phi_1}{\partial \chi} + Q\frac{\partial^3 \phi_1}{\partial \chi^3} + S\frac{\partial}{\partial \chi}\left(\frac{\partial^2 \phi_1}{\partial \xi^2} + \frac{\partial^2 \phi_1}{\partial \eta^2}\right) = 0. \tag{17}
$$

This is the trapped Zakharov–Kuznetsov (tZK) equation that accounts for the fractional nonlinearity due to the electron trapping effect, modifying the propagation of nonlinear waves. Here, the coefficients of fractional nonlinearity P, dispersion Q and S are defined, respectively, as

$$
P = -\frac{3}{2}\frac{B}{X_1},\ Q = \frac{1}{X_1},\ \text{and}\ S = \frac{X_2}{X_1}. \tag{18}
$$

with

$$
X_1 = \frac{2\lambda}{(\lambda^2 - 3\alpha\sigma_c)^2} + \frac{2\alpha(\lambda - v_{b0})}{\beta((\lambda - v_{b0})^2 - 3\alpha\sigma_b)^2}, \tag{19}
$$

and

$$
X_2 = 1 + \frac{1}{\Omega^2}\left(\frac{\lambda^4}{(\lambda^2 - 3\alpha\sigma_c)^2} + \frac{\alpha(\lambda - v_{b0})^4}{\beta((\lambda - v_{b0})^2 - 3\alpha\sigma_b)^2}\right). \tag{20}
$$

Note that the dispersive term in the parallel direction of propagation (i.e., Q) arises entirely due to the Poisson's equation, whereas the dispersion along the perpendicular direction (i.e., with coefficient S) is also affected by an additional effect of magnetic field. Observe that the trapping parameter γ changes the nonlinearity coefficient P (through B) only, while the parameters of the beam electrons modify all the coefficients. Neglecting trapping effect, i.e.,$\gamma = 1$, the fractional nonlinearity vanishes in Eq. (17) and no solitons exist. In such a case, the above stretchings become invalid and one needs to construct new stretching for independent coordinates for the formation of solitary structures. In the absence of electron beam $v_{b0} \to 0$ and $\beta \to \infty$.

IV. PHASE PORTRAITS

It is well-known that the phase portrait analysis or bifurcation theory provides a qualitative analysis of a dynamical system, without evaluating an exact solution of the system. From the phase portraits, one may easily identify the impact of various plasma parameters on the system trajectories and equilibrium points for stability in the system. This can be investigated by first transforming Eq. (17) for the formation of a dynamical system. Thus, we assume that ϕ_1 depends only on the variable:

$$
\zeta = l_1\xi + l_2\eta + l_3\chi - u_0\tau, \tag{21}
$$

where l_1, l_2, and l_3 represent the direction cosines in the ξ, η and χ directions, such that $l_1^2 + l_2^2 + l_3^2 = 1$, respectively, and u_0 is the speed of transformed frame. After using above transformation and performing integration once, Eq. (17) is simplified to

$$
-u_0\phi_1 + \frac{2}{3}Pl_3\phi_1^{3/2} + Q_1l_3\frac{\partial^2 \phi_1}{\partial^2 \zeta} = 0. \tag{22}
$$

Note that $Q_1 = Ql_3^2 + R(1 - l_3^2)$ and the constant of integration becomes null under the vanishing boundary conditions, i.e., $\phi_1 \to 0$ and $\partial^2\phi_1/\partial\zeta^2 \to 0$ at $\zeta \to \pm\infty$. As a result, the dynamical system represents the following set of ordinary differential equations:

$$
\begin{cases}
\frac{d\phi_1}{d\zeta} = z,\\
\frac{dz}{d\zeta} = \phi_1(\frac{u_0}{Q_1l_3} - \frac{2P}{3Q_1}\phi_1^{1/2}).
\end{cases}
\tag{23}
$$

where z, ϕ_1, and ζ represent the velocity, position and time, respectively, while keeping in view the terminology of a mechanical system. The Hamiltonion of the system (23) can be derived by utilizing the Hamilton's equations $\partial H/\partial\phi_1 = -dz/d\zeta$, and $\partial H/\partial z = d\phi_1/d\zeta$, as

$$
H = \frac{z^2}{2} + V(\phi_1), \tag{24}
$$

where the Sagdeev potential is defined by

$$
V(\phi_1) = \frac{4P}{15Q_1}\phi_1^{5/2} - \frac{u_0}{2Q_1l_3}\phi_1^2. \tag{25}
$$

To find stationary points and stability of a dynamical system, there is a crucial role of the equilibrium points upon which the system does not exhibit any temporal variation. These points are found from (23) as $P_1 = (0,0)$ and $P_2 = \left(0, \left(\frac{3u_0}{2Pl_3}\right)^2\right)$. Moreover, the stability and type of fixed points (i.e. node, saddle, or spiral) can be determined by linearizing the system around each fixed point. So, the Jacobian matrix for the system Eq.(23) is given by:

$$
J = \begin{pmatrix} 0 & 1 \\ \frac{u_0}{Q_1l_3} - \frac{2P}{3Q_1}\phi_1^{1/2} & 0 \end{pmatrix}, \tag{26}
$$

and the eigenvalues by $\det\left(J - \acute{\lambda}I\right) = 0$, (with I being the identity matrix), obtaining.

$$
\acute{\lambda}_{1,2} = \pm\sqrt{\frac{u_0}{Q_1l_3} - \frac{2P}{3Q_1}\phi_1^{1/2}}. \tag{27}
$$

These eigenvalues are then analyzed for the fixed points P_1 and P_2. One obtains $\acute{\lambda}_{1,2}\Big|_{P_1} = \pm\sqrt{u_0/Q_1 l_3}$ at fixed point $(0,0)$ and $\acute{\lambda}_{1,2}\Big|_{P_2} = \pm\sqrt{-u_0/2Q_1 l_3}$ at $(0,(\frac{3u_0}{2Pl_3})^2)$. There are two situations for these eigenvalues: For instance, if $u_0/Q_1 l_3 > 0$, then $\acute{\lambda}_{1,2}\Big|_{P_1}$ acts as real, making P_1 the saddle point, whereas $\acute{\lambda}_{1,2}\Big|_{P_2}$ being the complex, making P_2 a centre point. Conversely, if $u_0/Q_1 l_3 < 0$, then P_1 acts as a centre point while P_2 gives a saddle point. However, Q_1 remains positive for all plasma parameters besides the velocity u_0 and direction cosine l_3, so later case is unphysical. Therefore, P_2 acts as a stable centre point for the closed elliptical trajectories. Additionally, the centre point P_2 may be located on the right or left of the saddle point P_1 corresponding to the compressive (positive hump) or rarefactive (negative dip) solitary waves. The EA waves generally characterized by the rarefactive solitons, but due to the presence of trapping effect in the present model, the equilibrium point contains squared value of $3u_0/2Pl_3$, which remains positive irrespective of the sign of nonlinearity coefficient P. Thus, the centre point lies on the right of the saddle point and consequently, leading to the compressive solitons. Furthermore, it is important to note that qualitative analysis also provides the periodic solutions besides the solitary waves for different initial conditions.

V. SOLITON SOLUTIONS

From the tZK equation (17), we find an exact soliton solution. For this purpose, we use the transformed Eq. (22) and integrate it under the vanishing boundary conditions at infinity of localized solution. As a result, the following soliton solution for the potential is obtained

$$\phi_1(\zeta) = \phi_m \mathrm{sech}^4\left(\frac{\zeta}{\Delta}\right), \tag{28}$$

where $\phi_m = (15u_0/8Pl_3)^2$ is the amplitude and $\Delta = 4\sqrt{Q_1 l_3/u_0}$ is the width of the soliton. We have noted that the soliton solution gives exactly the same graphical results as obtained by the qualitative analysis under correct boundary conditions. An EA soliton with positive potential appear due to the presence of superthermal trapped electrons. The corresponding electric field can be expressed into its components for complete analysis as

$$\vec{E}(\zeta) = \begin{pmatrix} E_\xi \hat{\xi} \\ E_\eta \hat{\eta} \\ E_\chi \hat{\chi} \end{pmatrix} = \begin{pmatrix} -\partial_\xi \phi_1 \hat{\xi} \\ -\partial_\eta \phi_1 \hat{\eta} \\ -\partial_\chi \phi_1 \hat{\chi} \end{pmatrix},$$

where, $\hat{\xi}$, $\hat{\eta}$ and $\hat{\chi}$ are unit vectors along the ξ, η, and χ directions. The electric field then becomes,

$$\vec{E}(\zeta) = \frac{4\phi_m}{\Delta}\mathrm{sech}^4\left(\frac{\zeta}{\Delta}\right)\tanh\left(\frac{\zeta}{\Delta}\right)(l_1\hat{\xi} + l_2\hat{\eta} + l_3\hat{\chi}). \tag{29}$$

The amplitude of the electric field is $|E| = (4\phi_m/\Delta)\sec h^4(\zeta/\Delta)\tanh(\zeta/\Delta)$ which corresponds to a bipolar electric field for the localized EA waves.

VI. RESULTS AND COMPARISON WITH OBSERVATIONS

The nonlinear effects play a significant role in the generation of BEN emissions, as observed by the Viking satellite in the aurora and other magnetospheric regions. The observations have shown solitary potential excitations associated with electric fields in the range from a few mV/m to $\sim 100mV/m$. In particular, Dubouloz et. al.[52] considered two short duration bursts of BEN emission at an altitude of about $10,000km$ in the dayside auroral zone, studying turbulence generated by the EA waves. The typical plasma parameters[53] involving burst b of the BEN emission are chosen here, namely $n_{c0} = 0.2cm^{-3}$, $n_{h0} = 1.5cm^{-3}$, $n_{b0} = 1cm^{-3}$, $T_h = 100eV$, and $T_c = T_b \sim 1eV$ with normalized values of $v_{b0} \sim 0.01 - 0.6$ for the beam velocity in the range $40 - 2000km/s$. Relying on these values, Singh et al.[53] have shown that the electric field associating the solitons are in the range $\sim 10 - 400mV/m$. For this burst α=7.5, β=1, σ_c=σ_b=0.01 which give $\phi_m \sim 35V$ and the width $\Delta \sim 75km$ for a hump shaped soliton. These values can be derived by un-normalizing the scaled variables, in which the maximum amplitude ϕ_m and width Δ are multiplied by T_h/e and λ_{dh}, respectively. Furthermore, Dubouloz et al.[52] considered the parameters of burst a with slightly higher densities of the cold and hot electrons, namely $n_{c0} = 0.5cm^{-3}$, $n_{h0} = 2.0cm^{-3}$, $n_{b0} = 1cm^{-3}$, $T_h = 250eV$ and $v_{b0} \sim 0 - 1$ for studying the EA waves with superthermal hot electrons. They showed a reduction in the electric field amplitude (i.e., $\sim 3 - 6mV/m$) in a magnetized plasma, while the amplitude ϕ_m and the width Δ of the soliton change to $\sim 100V$ and $\sim 35km$, respectively. This section corresponds to the parameters of the burst a of BEN in the dayside auroral region, investigating nonlinear properties of the EA waves in the presence of superthermal trapped hot electrons. Since trapping is a nonlinear phenomenon, it does not affect the linear EA wave modes, whereas the superthermality parameter significantly affects the waves modes.

For nonlinear investigation of EA waves, we analyze both the phase portraits and the soliton solutions. The phase portraits lead to the formation of solitary and periodic waves under specific initial conditions. On the other hand, the tZK equation is solved to obtain the potential and electric field of soliton solutions. Figure 2 (a) presents the phase portraits of the EA waves in the dayside auroral zone using the plasma parameters of the burst a from BEN, where an equilibrium point $P_2 = \left(0, \left(\frac{3u_0}{2Pl_3}\right)^2\right)$ acts as the center of closed curves. The closed curves follow elliptical or homoclinic trajectories and periodic trajectories. It is worth mentioning here that a homoclinic trajectory refers to a loop-like curve that leaves a specific fixed point (a saddle point) and eventually returns back to the same point. Hence, a homoclinic trajectory of a pseudoparticle first passes through the saddle point $P_1 = (0,0)$ with zero velocity, moves with a finite velocity $(\partial\phi_1/\partial\zeta)$ along the ϕ_1-axis and reaches back to the saddle point with negative velocity. The wave potential then starts to oscillate between the two zeros of the pseudo-Sagdeev potential. Furthermore, homoclinic and periodic trajectories occur on the

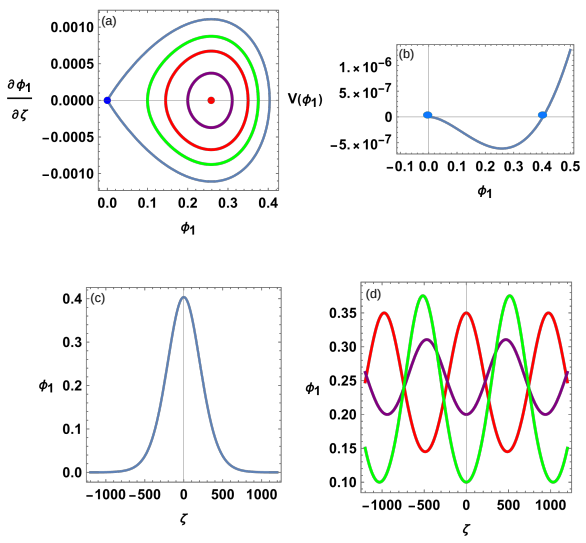

FIG. 2. Nonlinear EA waves exhibit different features showing (a) the phase portrait (pp) trajectories, (b) the Sagdeev potential curve, (c) the hump soliton profile (corresponding to blue curve in the pp), and (d) periodic wave profiles (identifying green, red and purple trajectories in the pp) for fixed values of α=4, β=2, v_{b0}=0.1, σ_c=0.001, σ_b=0.01, κ=2, ω=0.01, and γ=0.1.

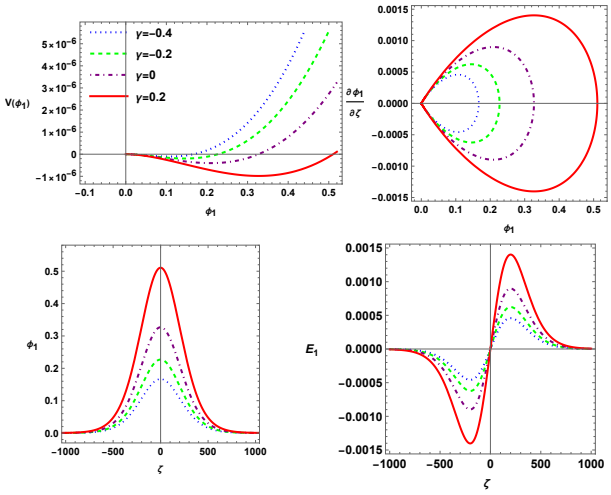

FIG. 3. Nonlinear features of EA waves are shown for different trapping parameter values, significantly affecting (a) The phase portraits, (b) The Sagdeev potential, (c) The corresponding solitary wave profile, and (d) The corresponding electric field profiles. Here, α=4, β=2, v_{b0}=0.1, σ_c=0.001, σ_b=0.01, κ=2, and ω=0.01.

positive ϕ_1-axis [see Fig. 2(a)], leading to the existence of compressive solitons and periodic waves with positive amplitude. Thus, the homoclinic trajectory passing through the saddle point $P_1 = (0,0)$ in Fig. 2(a) and the points indicated on the Sagdeev potential in Fig. 2(b) correspond to the formation of a compressive soliton pulse shown in Fig. 2(c). The width of the homoclinic trajectory along the ϕ_1-axis corresponds to the amplitude of the soliton while the depth of the Sagdeev potential determines the width of the soliton. It may also be noted that the amplitude of solitary structures remains positive due to the presence of electron trapping, therefore the phase trajectories only appear on the positive ϕ_1 axis.

On the other hand, different periodic trajectories in Fig 2(a) correspond to the periodic waves shown in Fig. 2(d) in the respective colors. In phase space representation, periodic waves are depicted as closed orbits around a stable center, demonstrating stable regular oscillations. These waves avoid passing through the saddle point in phase space and can be affected by superthermal trapped particles having a crucial role in maintaining the stability of periodic waves. However, we have observed that these phase trajectories are obtained for the fixed values of plasma parameters and the amplitude of the soliton may change with the values of plasma parameters, and the periodic waves rely on the initial conditions.

To illustrate numerically the impact of hot-electron trapping via the trapping parameter γ on the nonlinear profiles of EA waves, various distinct features including the Sagdeev potential, phase portraits, electric potential and electric field are depicted in Figs. 3(a-d). See that the depth and amplitude of the Sagdeev potential are strongly influenced by the variation of trapping parameter γ in Fig. 3(a). The phase portraits are shown in Fig. 3(b), representing a graphical view of the dynamical system for various values of γ. The shape of the homoclinic trajectories changes and contributes to the amplitude and width of the soliton structure. The potential curves shown in Fig. 3(c) represent a significant modification caused by the variation of trapping efficiency of hot electrons. Here, the case $\gamma < 0$ would be of vital interest for the vortex distribution. The maximum amplitude of the electric potential is obtained for positive trapping parameter, and as the trapping parameter γ becomes more and more negative, the magnitude of potential amplitude reduces accordingly. This happens because the trapping parameter only affects the nonlinearity coefficient P via B, keeping the dispersion terms unchanged. Thus, the amplitude of the soliton being inversely proportional to the nonlinearity coefficient, reduces with more negative values of γ and consequently solitons become shorter. The corresponding bipolar electric field is plotted in Fig 3(d), where an unnormalized amplitude of the electric field ranges $\sim 2.7 - 8.4 mV/m$.

Figures 4(a-d) display how superthermality index κ modifies the qualitative and quantitative characteristics of the EA soliton. It is clear that increase of spectral index κ leads to enhancement of amplitude of the potential of solitary structures. However, increasing κ tantamounts to decreasing the superthermal electrons, so lower amplitudes correspond to higher superthermality. The corresponding electric field amplitude varies from $4.0 mV/m$ to $4.8 mV/m$ in Fig. 4(d). It may also be deduced from the plot that as the distribution function approaches the Schamel's distribution function for $\kappa \to \infty$, we get the soliton of maximum amplitude. However, one cannot reduce these results to the pure Maxwellian distributed electrons, i.e., $\kappa \to \infty$ and $\gamma \to 1$, since the nonlinearity vanishes at $\gamma = 1$ and the stretching then needs to be changed for Maxwellian plasmas.

The nonlinear characteristics of the EA solitons are illus-

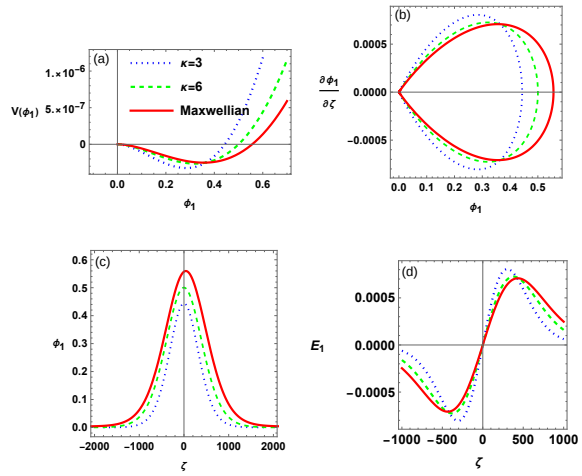

FIG. 4. Nonlinear features of the EA waves such as (a) phase portraits, (b) Sagdeev potential, (c) corresponding solitary wave profiles, and (d) corresponding electric field profiles, are influenced by the variation of superthermality parameter κ. Here, α=4, β=2, v_{b0}=0.1, σ_c=0.001, σ_b=0.01, γ=0.1, and ω=0.01.

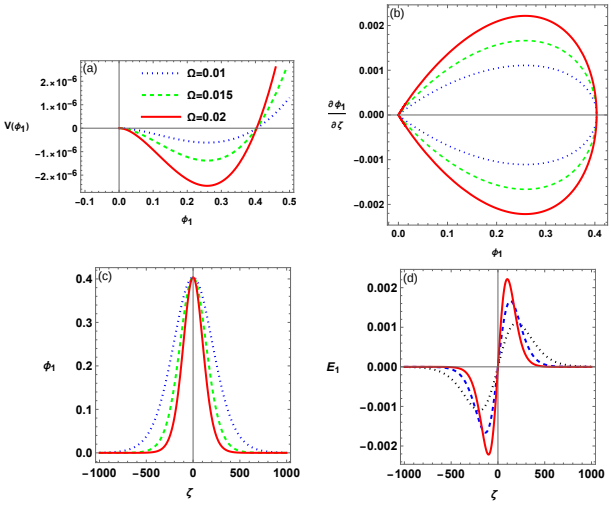

FIG. 5. Nonlinear features of the EA waves such as (a) Phase portraits, (b) Sagdeev potential, (c) The corresponding solitary wave profile, and (d) The corresponding electric field profiles are shown with variation of magnetic field parameter Ω. Here, α=4, β=2, v_{b0}=0.1, σ_c=0.001, σ_b=0.01, γ=0.1, and κ=2.

trated by Figs. 5(a-d) for varying the background magnetic field effect. In this respect, the profiles of the Sagdeev potential, homoclinic trajectories, and the electric potential are shown in Figs. 5(a-c). It is found that the amplitude of solitary waves remains unchanged, while the width of the wave reduces with the increase of background magnetic field. Here, it is important to mention that the coefficient Q of the dispersion term in the ZK equation does not depend on the magnetic field, so both the amplitude and width will remain unchanged along the parallel direction of propagation. On the other hand, the dispersion along the perpendicular direction of propagation involving the coefficient S is strongly influenced by the magnetic field through Ω, effectively changing the width of the soliton. Furthermore, the curves of the electric field, see Fig. 5(d) show a change with magnetic field. Since the electric field is essentially the negative slope of the electric potential, therefore, the slope for the maximum potential becomes zero and consequently the electric field vanishes for all curves, while the soliton potential with a smaller width has greater slope, thus the shape of electric field curves is obtained with the electric field amplitude varying from $6.3mV/m - 13.3mV/m$.

Next, we observe how the beam parameters alter the properties of EA solitons as clearly shown in Fig. 6. The Fig. 6(a) illustrates the impact of beam speed v_{b0} on the EA soliton in a trapped superthermal plasma. Note that as the beam streaming velocity is enhanced, the soliton amplitude becomes pronounced. Here, the velocity of the beam electrons contribute as a source of free energy, thus enhancing the amplitude of solitons. The effect of number density of beam electrons on the EA waves is depicted in Fig. 6(b) through the parameter β, which enhances the amplitude of solitons. However, an increase of β value is equivalent to a decrease of beam number density, therefore there is a net reduction of amplitude of EA soliton with the increase of beam density from $(0.9 - 1.1)cm^{-3}$. Figure 6(c) delineates the effect of beam temperature through the parameter σ_b on the solitary structure with superthermal trapped electrons. It is apparent from the plot that enhancement of the beam temperature $0eV$-to-$25eV$ leads to increase the electric potential. Thus, at lower value of σ_b, shorter and narrower solitons are formed, while at higher value of σ_b the potential pulses become taller and wider.

In Figs. 7(a-b), we show how the cold electron density and cold electron temperature affect the solitary structures of EA waves. With the increase of hot-to-cold beam electron density ratio $\alpha(\equiv n_{h0}/n_{c0})$, the amplitude of solitons reduces which results into the enhancement of soliton amplitude with the increasing density of cold electrons. This is in accordance with the fact that EA waves are associated with the enhancement of dynamical cold electrons and reduction of finite (more than $\sim 20\%$) hot electrons. The effect of cold electron temperature is depicted in Figure 7(b) through the ratio of cold-to-hot electron temperature σ_c, which shows that the amplitude of soliton is enhanced with increasing temperature of cold electrons.

It is worth mentioning that the parametric range of the electric field associated with the EA solitons is well-agreed with observational data[8], where the parallel electric field varies upto $100mV/m$. For the case of burst a, the electric field of solitary structures in the presence of magnetic field reduces to $\sim 15mV/m$ in accordance with the results of Singh et al.[43]. This value is much lesser than the magnitude of bipolar electric fields for electrostatic waves in an un-magnetized plasma[54]. Therefore, the present model is valid to explain electrostatic solitary structures during BEN emissions in auroral region of Earth's magnetosphere. The study has advanced existing research by modeling superthermal trapped hot elec-

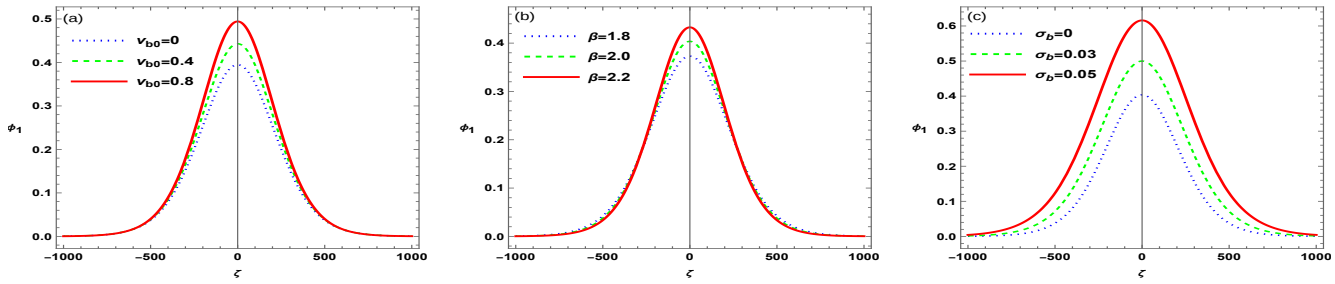

FIG. 6. The electric potential of EA solitons versus the spatial coordinate for varying (a) the beam velocity (for β=2, and σ_b=0.01) (b) the hot-to-beam electron density ratio (for v_{b0}=0.1, and σ_b=0.01) and (c) the beam-to-hot electron temperature ratio (for β=2, and v_{b0}=0.1). Here, α=4, σ_c=0.001, κ=2, ω=0.01, and γ=0.1.

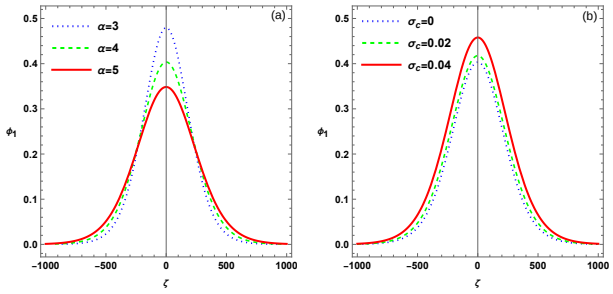

FIG. 7. The electric potential of EA waves is plotted against the spatial coordinate for changing (a) the hot-to-cold beam electron density ratio (for σ_c=0.001) and (b) cold-to-hot electron tamperature ratio (for α=4). Here, β=2, v_{b0}=0.1, σ_b=0.01, κ=2, ω=0.01, and γ=0.1.

trons to better represent the auroral region and identified various new features of phase portraits involving the tZK solitons. The model has relevance to understand transport of energy and momentum between plasma particles, electron dynamics, and plasma turbulence in auroral region of Earth's magnetosphere. Future perspectives of this work include investigations of long wavelength perturbations and instabilities at different timescales in dispersive and dissipative plasmas. In addition, interaction of nonlinear coherent structures will be studied to explain phase shifts, and formation of bipolar and tripolar electric fields in the presence of beam electrons.

VII. CONCLUSION

To conclude, we have presented the linear and nonlinear properties of the electron acoustic (EA) waves in a four component magnetoplasma, containing cold inertial electrons, superthermal (hot) trapped electrons and static ions with warm drifting beam electrons. In linear analysis, quartic roots in terms of linear phase speed are analysed with the variation of superthermality index κ. For nonlinear features of EA waves, fluid equations are solved by using the reductive perturbation technique, obtaining a trapped Zakharov Kuznetsov (tZK) equation. The latter is analyzed both qualitatively and quantatively. In qualitative analysis, the EA waves produce phase portraits and Sagdeev potential whereas quantitative analysis leads to the soliton solution of tZK equation under the dependent variable transformation technique. A positive potential pulse is produced due to trapping effect which corresponds to the hole for cold electron density. The soliton solution is numerically analyzed for plasma parameters of short burst of BEN emission in auroral region, varying the trapping efficiency γ and superthermality κ. It may be noted that particle trapping (superthermality) leads to reduction (enhancement) of pulse amplitude of EA soliton. A parametric analysis is carried out to examine the impact of parameters such as drifting speed, temperature and density of beam electrons, and temperature and density of cold electrons on the characteristics of EA solitons. The electric fields associated with solitary structures reveal a good agreement with observed data of auroral region. This model can also be applied to magnetopause, where two temperature electrons and large-amplitude parallel electrostatic waves exist, reported by MMS observations.

VIII. DATA AVAILABILITY STATEMENT

All data that supports the findings of this study are included within the article.

[1]B. D. Fried and R. W. Gould, "Longitudinal ion oscillations in a hot plasma," Physics of Fluids **4**, 139 (1961).
[2]D. Henry and J. Trguier, "Propagation of electronic longitudinal modes in a non-maxwellian plasma," Journal of Plasma Physics **8**, 311–319 (1972).
[3]S. P. Gary and R. L. Tokar, "The electron-acoustic mode," The Physics of fluids **28**, 2439–2441 (1985).
[4]M. Temerin, K. Cerny, W. Lotko, and F. Mozer, "Observations of double layers and solitary waves in the auroral plasma," Physical Review Letters **48**, 1175 (1982).
[5]V. Angelopoulos, D. Sibeck, C. Carlson, J. McFadden, D. Larson, R. Lin, J. Bonnell, F. Mozer, R. Ergun, C. Cully, *et al.*, "First results from the themis mission," Space Science Reviews **141**, 453–476 (2008).
[6]R. L. Tokar and S. P. Gary, "Electrostatic hiss and the beam driven electron acoustic instability in the dayside polar cusp," Geophysical Research Letters **11**, 1180–1183 (1984).
[7]R. Boström, B. Holback, G. Holmgren, and H. Koskinen, "Solitary structures in the magnetospheric plasma observed by viking," Physica Scripta **39**, 782 (1989).
[8]R. Ergun, C. Carlson, J. McFadden, F. Mozer, G. Delory, W. Peria, C. Chaston, M. Temerin, I. Roth, L. Muschietti, *et al.*, "Fast satellite observations

of large-amplitude solitary structures," Geophysical Research Letters **25**, 2041–2044 (1998).
[9]R. Pottelette, R. Ergun, R. Treumann, M. Berthomier, C. Carlson, J. McFadden, and I. Roth, "Modulated electron-acoustic waves in auroral density cavities: Fast observations," Geophysical Research Letters **26**, 2629–2632 (1999).
[10]H. Matsumoto, H. Kojima, T. Miyatake, Y. Omura, M. Okada, I. Nagano, and M. Tsutsui, "Electrostatic solitary waves (esw) in the magnetotail: Ben wave forms observed by geotail," Geophysical Research Letters **21**, 2915–2918 (1994).
[11]J. Pickett, S. Kahler, L.-J. Chen, R. Huff, O. Santolik, Y. Khotyaintsev, P. Décréau, D. Winningham, R. Frahm, M. Goldstein, *et al.*, "Solitary waves observed in the auroral zone: the cluster multi-spacecraft perspective," Nonlinear Processes in Geophysics **11**, 183–196 (2004).
[12]D. B. Graham, Y. V. Khotyaintsev, A. Vaivads, and M. André, "Electrostatic solitary waves with distinct speeds associated with asymmetric reconnection," Geophysical Research Letters **42**, 215–224 (2015).
[13]F. Scarf, L. Frank, K. Ackerson, and R. Lepping, "Plasma wave turbulence at distant crossings of the plasma sheet boundaries and the neutral sheet," Geophysical Research Letters **1**, 189–192 (1974).
[14]D. A. Gurnett, "Plasma wave interactions with energetic ions near the magnetic equator," Journal of Geophysical Research **81**, 2765–2770 (1976).
[15]N. Dubouloz, R. Pottelette, M. Malingre, and R. Treumann, "Generation of broadband electrostatic noise by electron acoustic solitons," Geophysical Research Letters **18**, 155–158 (1991).
[16]G. Lakhina, S. Singh, A. Kakad, and J. Pickett, "Generation of electrostatic solitary waves in the plasma sheet boundary layer," Journal of Geophysical Research: Space Physics **116**, A10218 (2011).
[17]C. Dillard, I. Vasko, F. Mozer, O. Agapitov, and J. Bonnell, "Electron-acoustic solitary waves in the earth's inner magnetosphere," Physics of Plasmas **25**, 022905 (1–9) (2018).
[18]R. Ergun, J. Holmes, K. Goodrich, F. Wilder, J. Stawarz, S. Eriksson, D. Newman, S. Schwartz, M. Goldman, A. Sturner, *et al.*, "Magnetospheric multiscale observations of large-amplitude, parallel, electrostatic waves associated with magnetic reconnection at the magnetopause," Geophysical Research Letters **43**, 5626–5634 (2016).
[19]D. B. Graham, A. Vaivads, Y. V. Khotyaintsev, M. André, O. Le Contel, D. Malaspina, P.-A. Lindqvist, F. Wilder, R. Ergun, D. Gershman, *et al.*, "Large-amplitude high-frequency waves at earth's magnetopause," Journal of Geophysical Research: Space Physics **123**, 2630–2657 (2018).
[20]J.-P. Lynov, P. Michelsen, H. Pécseli, J. J. Rasmussen, K. Saeki, and V. Turikov, "Observations of solitary structures in a magnetized, plasma loaded waveguide," Physica Scripta **20**, 328 (1979).
[21]M. Goldman, D. Newman, and R. Ergun, "Phase-space holes due to electron and ion beams accelerated by a current-driven potential ramp," Nonlinear Processes in Geophysics **10**, 37–44 (2003).
[22]P. Guio, S. Børve, L. Daldorff, J.-P. Lynov, P. Michelsen, H. Pécseli, J. Juul Rasmussen, K. Saeki, and J. Trulsen, "Phase space vortices in collisionless plasmas," Nonlinear processes in geophysics **10**, 75–86 (2003).
[23]J. Moody and C. Driscoll, "Rarefaction waves, solitons, and holes in a pure electron plasma," Physics of Plasmas **2**, 4482–4493 (1995).
[24]C. Cattell, C. Neiman, J. Dombeck, J. Crumley, J. Wygant, C. Kletzing, W. Peterson, F. Mozer, and M. André, "Large amplitude solitary waves in and near the earth's magnetosphere, magnetopause and bow shock: Polar and cluster observations," Nonlinear Processes in Geophysics **10**, 13–26 (2003).
[25]R. Ergun, L. Andersson, D. Main, Y.-J. Su, D. Newman, M. Goldman, C. Carlson, J. McFadden, and F. Mozer, "Parallel electric fields in the upward current region of the aurora: Numerical solutions," Physics of Plasmas **9**, 3695–3704 (2002).
[26]L. Andersson, R. E. Ergun, D. L. Newman, J. P. McFadden, C. W. Carlson, and Y.-J. Su, "Characteristics of parallel electric fields in the downward current region of the aurora," Physics of plasmas **9**, 3600–3609 (2002).
[27]F. Mozer, O. Agapitov, A. Artemyev, J. Drake, V. Krasnoselskikh, S. Lejosne, and I. Vasko, "Time domain structures: What and where they are, what they do, and how they are made," Geophysical Research Letters **42**, 3627–3638 (2015).
[28]I. B. Bernstein, J. M. Greene, and M. D. Kruskal, "Exact nonlinear plasma oscillations," Physical Review **108**, 546 (1957).
[29]H. Schamel, "Stationary solitary, snoidal and sinusoidal ion acoustic waves," Plasma Physics **14**, 905 (1972).
[30]H. Schamel, "A modified korteweg-de vries equation for ion acoustic wavess due to resonant electrons," Journal of Plasma Physics **9**, 377–387 (1973).
[31]F. Verheest and W. Hereman, "Conservations laws and solitary wave solutions for generalized schamel equations," Physica Scripta **50**, 611 (1994).
[32]A. A. Mamun and P. K. Shukla, "Electron-acoustic solitary waves via vortex electron distribution," Journal of Geophysical Research: Space Physics **107**, SIA–15 (2002).
[33]A. A. Mamun, P. K. Shukla, and L. Stenflo, "Obliquely propagating electron-acoustic solitary waves," physics of plasmas **9**, 1474–1477 (2002).
[34]O. R. Rufai, G. V. Khazanov, and S. Singh, "Finite amplitude electron-acoustic waves in the electron diffusion region," Results in Physics **24**, 104041 (2021).
[35]H. Demiray, "A note on the cylindrical waves with transverse distortion in a plasma with vortex electron distribution," TWMS Journal of Applied and Engineering Mathematics **10**, 685 (2020).
[36]S. Guo, L. Mei, Y.-L. He, H. Guo, and Y. Zhao, "The effect of trapped electrons on the three-dimensional ion-acoustic shock wave in magnetized ionic-pair plasma," Europhysics Letters **114**, 25002 (2016).
[37]H. Schamel, "Theory of electron holes," Physica Scripta **20**, 336 (1979).
[38]G. Williams, F. Verheest, M. Hellberg, M. Anowar, and I. Kourakis, "A schamel equation for ion acoustic waves in superthermal plasmas," Physics of Plasmas **21**, 092103 (2014).
[39]S. Sultana, A. Mannan, and R. Schlickeiser, "Obliquely propagating electron-acoustic solitary waves in magnetized plasmas: The role of trapped superthermal electrons," The European Physical Journal D **73**, 1–8 (2019).
[40]D. Montgomery, R. Focia, H. Rose, D. Russell, J. Cobble, J. Fernández, and R. Johnson, "Observation of stimulated electron-acoustic-wave scattering," Physical Review Letters **87**, 155001 (2001).
[41]M. Berthomier, R. Pottelette, M. Malingre, and Y. Khotyaintsev, "Electron-acoustic solitons in an electron-beam plasma system," Physics of Plasmas **7**, 2987–2994 (2000).
[42]W. El-Taibany and W. M. Moslem, "Higher-order nonlinearity of electron-acoustic solitary waves with vortex-like electron distribution and electron beam," Physics of plasmas **12**, 032307 (2005).
[43]S. Singh, S. Devanandhan, G. Lakhina, and R. Bharuthram, "Electron acoustic solitary waves in a magnetized plasma with nonthermal electrons and an electron beam," Physics of Plasmas **23**, 082310 (2016).
[44]U. Kumar Samanta, A. Saha, and P. Chatterjee, "Bifurcations of dust ion acoustic travelling waves in a magnetized dusty plasma with a q-nonextensive electron velocity distribution," Physics of Plasmas **20**, 022111 (2013).
[45]R. Shahein and A. R. Seadawy, "Bifurcation analysis of kp and modified kp equations in an unmagnetized dust plasma with nonthermal distributed multi-temperatures ions," Indian Journal of Physics **93**, 941–949 (2019).
[46]S. Ali, W. Masood, H. Rizvi, R. Jahangir, and A. M. Mirza, "Contribution of the generalized (r, q) distributed electrons in the formation of nonlinear ion acoustic waves in upper ionospheric plasmas," AIP Advances **11**, 125020 (2021).
[47]Y. Wu and Z. Liu, "New types of nonlinear waves and bifurcation phenomena in schamel-korteweg-de vries equation," in *Abstract and Applied Analysis*, Vol. 2013 (Wiley Online Library, 2013) p. 483492.
[48]J. Tamang and A. Saha, "Phase plane analysis of the dust-acoustic waves for the burgers equation in a strongly coupled dusty plasma," Indian Journal of Physics **95**, 749–757 (2021).
[49]M. Hafez, P. Akter, K. Chettri, R. Sakthivel, and A. Saha, "Nonlinear propagation of ion-acoustic waves along with their bifurcation analysis in a negative ion plasma in the presence of quartic nonlinearity," Physics of Fluids **36**, 077170 (2024).
[50]H. Washimi and T. Taniuti, "Propagation of ion-acoustic solitary waves of small amplitude," Physical Review Letters **17**, 996 (1966).
[51]R. Jahangir and S. Ali, "Interaction of beam-driven electron-acoustic solitons in auroral region," in *Emerging Applications of Plasma Science in Allied Technologies* (IGI Global, 2024) pp. 175–209.
[52]N. Dubouloz, R. Treumann, R. Pottelette, and M. Malingre, "Turbulence generated by a gas of electron acoustic solitons," Journal of Geophysical Research: Space Physics **98**, 17415–17422 (1993).

[53]S. Singh and G. Lakhina, "Generation of electron-acoustic waves in the magnetosphere," Planetary and Space Science **49**, 107–114 (2001).

[54]R. Jahangir, W. Masood, and H. Rizvi, "Interaction of electron acoustic solitons in auroral region for an electron beam plasma system," Frontiers in Astronomy and Space Sciences **9**, 978314 (2022).